AD NUMBER
AD389124
LIMITATION CHANGES

TO:

Approved for public release; distribution is unlimited.

FROM:

Distribution authorized to U.S. Gov't. agencies and their contractors; Administrative/Operational Use; APR 1968. Other requests shall be referred to Arnold Engineering Development Center, Arnold AFB, TN.

AUTHORITY

AEDC ltr 15 Oct 1975

AEDC-TR-67-257

DECLASSIFIED / UNCLASSIFIED

EXPERIMENTAL STUDY OF FLOW GEOMETRY AND TRANSITION IN THE NEAR WAKE OF A SHARP SLENDER CONE (U)

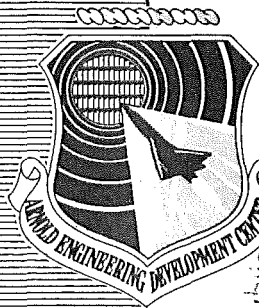K. E. Koch

ARO, Inc.

April 1968

In addition to security requirements which must be met, this document is subject to special export controls and each transmittal to foreign governments or foreign nationals may be made only with prior approval of Arnold Engineering Development Center (AETS), Arnold AF Station, Tennessee 37389.

This material contains information affecting the national defense of the United States within the meaning of the Espionage Laws (Title 18, U.S.C., sections 793 and 794). the transmission or revelation of which in any manner to an unauthorized person is prohibited by law.

VON KÁRMÁN GAS DYNAMICS FACILITY
ARNOLD ENGINEERING DEVELOPMENT CENTER
AIR FORCE SYSTEMS COMMAND
ARNOLD AIR FORCE STATION, TENNESSEE

DECLASSIFIED / UNCLASSIFIED

NOTICES

This document has been approved for public release, its distribution is unlimited. *Per AF Letter*

15 October 1975

Signed William O. Coke

UNCLASSIFIED

EXPERIMENTAL STUDY OF FLOW GEOMETRY AND
TRANSITION IN THE NEAR WAKE OF A
SHARP SLENDER CONE (U)

K. E. Koch

ARO, Inc.

This document has been approved for public release,
its distribution is unlimited.

This material contains information affecting the
national defense of the United States the
meaning of the Espionage Law Title 18, U.S.C.,
sections 793 and transmission or revelation
of which manner to an unauthorized person is
prohibited by law.

NATIONAL SECURITY INFORMATION
Unauthorized Disclosure Subject
to Criminal Sanctions

UNCLASSIFIED

DECLASSIFIED / UNCLASSIFIED

FOREWORD

(U) The work reported herein was sponsored by the Arnold Engineering Development Center (AEDC), Air Force Systems Command (AFSC), under Program Element 6240533F, Project 8953, Task 895309.

(U) The results of research presented were obtained by ARO, Inc. (a subsidiary of Sverdrup & Parcel and Associates, Inc.), contract operator of the AEDC, AFSC, Arnold Air Force Station, Tennessee, under Contract AF40(600)-1200. The research was conducted from September 1, 1966, to February 1, 1967, under ARO Project Nos. VT2711-K00 and VT2727-K00, and the manuscript was submitted for publication on November 3, 1967.

(U) The author wishes to express his appreciation to O. H. Bock, of the Aerophysics Branch, who designed and developed the schlieren systems used to obtain these data.

(U) This report contains no classified information extracted from other classified documents.

(U) This report has been reviewed and is approved.

Carl E. Simmons
Captain, USAF
Research Division
Directorate of Plans
  and Technology

Edward R. Feicht
Colonel, USAF
Director of Plans
  and Technology

DECLASSIFIED / UNCLASSIFIED

This page is Unclassified

DECLASSIFIED / UNCLASSIFIED

CONFIDENTIAL ABSTRACT

(C) This is a report of an investigation of that region of the wake
of a cone at supersonic speeds and zero angle of attack lying between
the base of the cone and the portion of the wake where the free shear
layer has converged on the axis of symmetry. Downstream of this
region, local static pressures equal the free-stream value. Sharp-
nosed cones of 10-deg half-angle at Mach numbers near 5 were
launched in an aeroballistics range to furnish data for this study. It
has been shown that when the location of transition from laminar to
turbulent flow occurs in the free shear layer, it is not at a position
fixed with respect to the body, but occurs ahead of the wake minimum
cross section or neck. The neck, in turn, moves downstream as the
free-stream Reynolds number is decreased. For the lowest Reynolds
number of these experiments, the neck was located more than 9 base
diameters behind the cone base, whereas it was less than 2 diameters
from the base at the highest Reynolds numbers. It is suggested that
the neck plays a strong part in controlling the location of transition in
the near wake. The shape of the lip shock near the base was shown to
be independent of free-stream Reynolds number for the range of
Reynolds numbers covered.

This document has been approved for public release
its distribution is unlimited.

DECLASSIFIED / UNCLASSIFIED

The reverse side of this page is blank.

UNCLASSIFIED

CONTENTS

APPENDIXES

I.   ILLUSTRATIONS

Figure

NOMENCLATURE

C_D	Drag coefficient
D	Body base diameter, in.
L	Body axial length, in.
L'	Trajectory length, ft
M	Mach number

r	Distance measured in radial direction, in.
Re	Reynolds number
T	Temperature, °K
U	Free-stream velocity, ft/sec
w	Wake neck diameter, in.
X	Axial distance
X_n	Distance to wake neck, measured from nose, in.
X_{TR}	Distance to transition, measured from nose, in. (see Fig. 3)
z	Distance along trajectory, ft
α	Angle of attack of model in plane of individual photographs, deg
δ	Local total angle of attack, deg
$\overline{\delta^2}$	Mean squared total angle of attack, $\deg^2$ (defined by Eq. (1)
θ	Model half-angle, deg
ρ_∞	Mass density of range air, slugs/ft^3
Φ	Wake closure half-angle, deg

SUBSCRIPTS

aw	Adiabatic wall conditions
D	Using cone base diameter as reference length
o	Zero angle of attack
w	Model wall conditions
X_n	Using X_n as reference length
X_{TR}	Using X_{TR} as reference length
∞	Free-stream conditions

SECTION I
INTRODUCTION

(U) The survey papers concerned with hypersonic flow fields by Cheng (Ref. 1) and Lykoudis (Ref. 2) state that among the areas requiring extensive experimental investigation is the base flow region for laminar, transitional, and fully turbulent flow conditions. Many mathematical approaches, discussed briefly in Refs. 1 and 2, have been developed for analysis of the near wake (i. e. , the flow region extending from the base downstream past the wake neck to the region where the local pressure has returned to the free-stream value). These investigations have shown that the primary source for high temperature fluid in the wake of a sharp slender body is the boundary layer. They indicate that the character of the far wake is controlled by the manner in which the boundary layer is processed through the base flow region, together with the location of transition from laminar to turbulent flow.

(U) Wilson (Ref. 3) using an aeroballistic range, has shown that for hypersonic blunt bodies the location of transition will move upstream with increasing Reynolds number and eventually "stick" (i. e. , occur at a position in the wake fixed with respect to the body) just downstream of the wake neck. As the Reynolds number is increased further, transition will finally jump forward onto the body. This was not seen for sharp bodies at $M_\infty \approx 20$ and $Re_{\infty, D} < 6.3 \times 10^5$. However, for these $M_\infty \approx 20$ conditions, the location of transition was never closer to the body than 30 diameters so that its behavior in the vicinity of the body base was not observed.

(U) This phenomena of "sticking" for sharp bodies has recently been investigated by Bailey (Ref. 4) where it is also shown that "sticking" does not exist under the conditions investigated, which included a wide variation of M_∞ and several cone geometries.

(U) The present investigation was carried out to study the character of the base flow region as transition moved from the body to the near wake. All of the data were obtained in aeroballistic ranges. The primary instrumentation consisted of sensitive schlieren systems. Appendix III contains a brief description of the ranges used. The use of aeroballistic ranges together with the schlieren systems allowed observation of the flow field over a range of more than two orders of magnitude of Reynolds number at a fixed Mach number (and velocity) and fixed model size. The test gas was air with a nominal free-stream temperature of 300°K. The study was conducted at a nominal free-stream Mach number of 5.2. This kept flow field temperatures relatively low in order to minimize flow field

chemistry effects on the phenomenon under investigation. Further, since the average model wall temperature did not change because of the short time of flight, $T_w/T_{aw} = 0.18$. Also, at this Mach number, the bow shock did not lie so close to the body as to interfere with schlieren observations of the boundary layer and near wake flow.

(U) Sketches of the models and sabots used in this investigation are shown in Figs. 1 and 2. The surface finish on all models was $12-\mu$ in. rms or better. All model noses were viewed and photographed on a comparator which provided a 100X enlargement to determine the exact shape of the nose. Prior to launching, each model was cleaned in an ultrasonic Freon Precision Cleaning Agent bath.

(U) The first design of the 1.75-in. base diameter model was a scaled-up version of model B, but with a sealed base, and will be referred to as model B_1. The 0.30-in. base diameter multimetal model will be referred to as model B_2. The initial shots using model B_1 showed that local shocks were occurring at the locations of the joints. It was suspected that an upsetting of the joints was occurring during the launch, even though there was no measurable surface discontinuity visible on the cones. The upsets were considered undesirable because of their possible tripping of the boundary layer. In the range of Reynolds number where these local shocks were seen ($Re_{\infty, D} > 2.0 \times 10^6$), natural transition was on the body. For $Re_{\infty, D} < 8.0 \times 10^5$, no shock waves were seen on the body, and the boundary layer was completely laminar. Based on comparison with data from smooth models, shown later, the upsets had no effect on the location of transition or the geometry of the base flow field for these conditions.

(U) In order to avoid the problem of the joints, the design was changed to the one shown in Fig. 1, referred to as model A. The vent hole in the base was to provide a means of pressure relief so that the base bulkhead would not distort and to prevent any random leakage through the threads which would cause spurious results. Later in the program, prompted by concern over possible influence on the data, the time for venting the cavity was calculated and found to be much greater than the time of flight under some conditions. The venting mass flow rate under choked flow conditions was calculated to be 0.017 percent of the mass flow rate swept out by the model, i.e., $\rho_\infty U_\infty \pi D^2/4$, assuming the cavity in the model was initially at the blast tank pressure. Fortunately, comparison of the data obtained from all of the models, including a number not having vented base bulkheads, indicates that the vent hole in the base of model A had no effect on the flow field geometry or the location of transition.

SECTION II
ANALYSIS OF TRANSITION DATA

(U) The models were launched at a nominal velocity of 5700 fps.
The range pressure was varied between 730 and 5 mm Hg. This corre-
sponds to a free-stream body base Reynolds number variation of
4.64×10^6 to 3.71×10^4 for the 1.75-in. base diameter cones. Table I
lists the various parameters measured on each shot. Figure 3 is a
sketch of the flow field showing the measurements tabulated in Table I.
The mean squared angle of attack $(\overline{\delta^2})$ is defined by Eq. (1).

$$\overline{\delta^2} = \frac{1}{L'} \int_0^{L'} \delta^2 \, dz \qquad (1)$$

(U) It is well known that boundary-layer transition from laminar
flow to full turbulence occurs over a length equal to many boundary-
layer thicknesses, and a point of transition or transition location is an
ambiguous term. Similarly, when transition occurs off the body, it
requires many local characteristic thicknesses to proceed from fully
laminar flow through the region of laminar instabilities to fully devel-
oped turbulent flow. (This can require hundreds of body diameters
under some conditions.) Accordingly, when one refers to a transition
point or transition location, a definition is required. In this report,
the point of transition or transition location is that point in the boundary
layer, free shear layer, or wake where full turbulence is considered to
first exist. Figures 4 through 12 are a series of schlieren and shadow-
graph photographs of the models for a range of free-stream Reynolds
numbers with arrows indicating where the author considers full turbu-
lence to first exist. (It must be noted that the originals show more
detail than these reproductions. This is especially true of the color
schlieren photographs of low Reynolds number flows.) Because small
but finite angles of attack usually existed, and these caused X_{TR} values
to differ on opposite sides of the flow fields pictured, it was necessary
to distinguish between "windward" and "leeward" flow regions in giving
X_{TR} data. Each transition point for the present data represents the
arithmetic average of all windward measurements (schlieren and shadow-
graph) for that shot. All the data are contained within a band of ±10
percent of the mean value.

(U) Figure 13 presents transition Reynolds number, based on free-
stream conditions and length X_{TR}, as a function of free-stream body
Reynolds number. Wake transition measurements obtained with a
similar model under similar flight conditions (Ref. 5) are compared
with the present data. To illustrate the relation of transition location
with the neck location, Re_{∞, X_n} is also plotted in Fig. 13.

(∅) The three data points at a body Reynolds number of 1.1×10^6 in Fig. 13 should be discussed separately since the transition location is very near to the body base at this condition. When individual windward and leeward measurements were plotted as a function of model angle of attack, as shown in Fig. 14, for each of three flights, a general trend of decreasing distance to transition with increasing angle of attack is seen for the leeward data. This is a result of a cross-flow which will thicken and destabilize the boundary layer on the leeward side. Browand et al. (Ref. 6) have indicated that a pair of vortices will be shed from the nose on the leeward side even at very small angles of attack (on the order of 8 percent of the cone half-angle). These would also cause instabilities in the boundary layer which would cause transition to move forward with increasing angle of attack. However, there appears to be little movement with angle of attack for the windward data. Transition on one shot (Fig. 14a) was consistently off the body in all photographs for angles as high as 2.5 deg. Windward data for the other two shots (Figs. 14b and c) were very inconsistent with angle of attack, appearing both on and off the body for angles of attack of 0.5 deg or larger. It can only be concluded that near to the base wake transition is very sensitive to slight variations in the local flow properties.

(∅) The discontinuity attributable to the sudden jump of transition as it moves off the body will be noted (Ref. 7). This discontinuity as transition leaves the body marks the beginning of the second region, i.e., transition in the separated wake upstream of the wake neck or closure. Transition is close behind the body and moves downstream very slowly as the Reynolds number is decreased. The phenomenon of transition "sticking" in the near wake, as shown to exist behind blunt bodies at high speeds (Ref. 3), is not demonstrated here, since transition sticking would be characterized by a straight line with a slope of 45 deg in Fig. 13.

(∅) The third region follows where transition moves downstream somewhat faster as the Reynolds number is decreased. Although it may be argued that the data could have also been fitted with a smooth curve instead of two straight lines, two slopes do exist in the data, and straight lines were drawn to emphasize this point. A possible reason for the two slopes will be discussed later. However, this region should be followed by a fourth region, not shown by the data, but suggested by Lees (Ref. 8). In this region, transition moves out rapidly to "infinity", and Lees has defined the Reynolds number at which this occurs as the "minimum critical" Reynolds number. For Reynolds numbers less than the "minimum critical" value, an instability in the wake would be damped out by the relatively strong viscous forces.

For the conditions of this test, Ref. 8 suggests that this Reynolds number is $1.0 \times 10^3 < Re_{\infty,D} < 2.0 \times 10^3$.

(C) Also shown in Fig. 13 is the axial position of the wake neck, represented by $Re_{\infty,Xn}$. The neck moves downstream with decreasing free-stream Reynolds number as can be seen by the slope of the curve. Of some interest is the fact that the neck is just downstream of the location of transition when X_{TR} lies in region two. Thus, transition is occurring in a convergent, nonisentropic flow of steep gradients in this second region. The process of formation of the neck is shown in Figs. 6 and 7. Figure 6 is a horizontal knife-edge schlieren photograph, and Fig. 7 is a vertical knife-edge photograph at the same flow conditions. At the lowest body Reynolds number (3.71×10^4), the resolution of the schlieren photographs is not sufficient to determine whether or not a neck existed. This neckless wake is not unique, but has been reported in Refs. 9 and 10. The free shear layer could be seen and appeared to have a constant diameter until turbulence appeared, when it began to increase in diameter. No neck shock could be seen in the flow field at this condition, but the apparent lip shock could be seen extending to at least 35 body diameters from the body base. At this point, the shocks were too far apart radially to be seen in the 30-in.-diam schlieren field of view. Figure 13 shows that the neck and location of transition tend to coincide for $Re_{\infty,D} \approx 10^5$ under present conditions.

(C) From the variation of the neck and transition locations with free-stream body Reynolds number, it is suggested that the recompression (and attendant local shocks as shown in Figs. 6 and 7) of the free shear layer controls the location of transition until the Reynolds number is low enough so that a neck does not exist. That is, the recompression gradient behind the body would become weak and would not enhance flow instability. For $Re_{\infty,D} < 10^5$, flow instabilities as discussed by Gold (Ref. 11) would control the location of transition. The Reynolds number where the neck location would no longer control the location of transition would presumably remain a function of other parameters, such as body shape and Mach number.

SECTION III
NEAR WAKE GEOMETRY

(U) During the study of the movement of transition from the body to the near wake region, it became evident that the neck geometry is a strong function of Reynolds number. Data correlated by Waldbusser (Refs. 12 and 13) have not shown such a strong effect.

(ϕ) In Fig. 15, the neck location is shown as a function of free-stream body Reynolds number. It is readily seen that as the free-stream Reynolds number is decreased, the neck moves downstream from the base. As mentioned before, at $Re_{\infty, D} \cong 3.7 \times 10^4$, the neck is very nebulous and difficult to define so that the position given in Fig. 15 represents what is considered to be the minimum distance that the neck can be from the body nose. The correlation shown in Refs. 12 and 13 implies that X_n is invariant with Reynolds number.

(ϕ) Figure 16 shows the neck diameter plotted as a function of free-stream body Reynolds number. For $Re_{\infty, D} > 10^6$, the neck diameter is constant and has a value of $w/D = 0.3$. For $Re_{\infty, D} < 10^6$, the neck diameter increases with decreasing body Reynolds number and reaches a value of almost $w/D = 0.8$ at the lowest Reynolds number tested. The data of Refs. 12 and 13 are similar to the present data in that they predict the same general growth rate, but yield a different diameter.

(ϕ) The wake closure angle is shown as a function of free-stream body Reynolds number in Fig. 17. This angle was measured at the midpoint of the distance between the body base and the neck. If the free shear layer is assumed to be straight, then the closure angle may be calculated from the measured neck diameter and its location as follows:

$$\Phi = \tan^{-1} \{[(1 - w/D)/2] / [X_n/D - 2.83]\} \qquad (2)$$

A comparison of the measured and calculated values of Φ indicates that the assumption of a straight shear layer will result in a value for Φ that is less than the measured value by about 2 deg when $Re_{\infty, D} < 1.2 \times 10^6$, or when transition occurs off the body. For $Re_{\infty, D} > 1.2 \times 10^6$, or when transition occurs on the body, the free shear layer is curving so steeply that it no longer is typified by one particular closure angle, and the straight line assumption breaks down. The data of Ref. 13 indicate a similar slope, but there is a shift of approximately 9 deg for equal M_{∞}. It must be recognized that accurate measurement of this angle is extremely difficult under some conditions, and a degree of individual judgement enters into its determination.

(ϕ) In order to show the physical relationship between free shear layer shape, neck location and size, and transition location, some of the photographs were used to construct a map of the base flow region. This is shown in Fig. 18 where the edge of the free shear layer and corresponding transition locations are shown in normalized coordinates with free-stream body Reynolds number as a parameter. What is

believed to be the lip shock also is indicated. This shock shape did not vary with Reynolds number for the range of Reynolds number covered, which is somewhat unexpected. It is interesting to note that what appears to be a second shock also was seen at the corner under some conditions, as shown in the photograph shown in Fig. 4 and the sketch shown in Fig. 19. This second shock was observed only for $Re_{\infty, D} > 1.4 \times 10^6$ and did not change shape for the very limited range of Reynolds number over which it was observed. The causes of this shock, if indeed it is a shock, are not known at present and in the absence of detailed wake surveys yielding local flow conditions it is possibly dangerous to speculate on the causes and nature of these apparent shocks. It can be shown that the final wave of the expansion fan originating at the cone base corner would nearly coincide with what is herein called the lip shock in many of these photographs.

(U) The near wake survey data of Ragsdale and Darling (Ref. 14) for a 9-deg half-angle cone suspended in the flow by a system of wires with an adiabatic wall at $M_{\infty} = 5$ and $Re_{\infty, D} = 3.2 \times 10^6$ show the bow shock, leading expansion wave, end of the expansion, and neck shock. There is no evidence of a lip shock. However, the data were obtained no closer to the base than 0.55 base diameter, and the lip shock may have been weakened by the expansion to the point where it could no longer be detected. Further, the schlieren photographs shown were obtained with a vertical knife-edge so that a nearly horizontal weak shock would probably not show up.

(U) Browand et al. (Ref. 6) have obtained wake survey data using a magnetic suspension system to support a 7-deg half-angle cone with $M_{\infty} = 4.3$ and $Re_{\infty, D} = 4.06 \times 10^4$ and an adiabatic wall. A weak lip shock is shown in the pitot profile data, but the Reynolds number is much too low to compare directly with the present data.

(U) Hama (Ref. 15) has conducted an extensive investigation of the lip shock on a 6-deg half-angle wedge with an adiabatic wall at free-stream Mach numbers from 2.01 to 4.54 and wedge surface Reynolds numbers from 3.75×10^5 to 4×10^4, based on base height. The data show that the lip shock orientation is a strong function of both Mach number and Reynolds number for the ranges covered. It was found that the lip shock had substantial strength and was apparently caused by viscous separation effects.

(U) Bauer (Ref. 16) has obtained pitot profiles behind a 12-deg half-angle cone at $M_{\infty} = 3.035$ and $Re_{\infty, D} = 1.13 \times 10^5$ that show a weak lip shock. The model was supported by a cantilevered strut extending upstream from the model nose.

(∅) Compared with the present data, the results of these other investigations indicate that (a) what is herein called the lip shock lies at a position consistent with the findings of Refs. 6 and 16, (b) the insensitivity of the lip shock to variations of free-stream Reynolds number reported here is at variance with the measurements for wedges reported in Ref. 15 and cannot be explained at this time, (c) location of the lip shock at the terminal boundary of the expansion fan noted in the present work is in agreement with Ref. 15, but this may not represent a general situation.

SECTION IV
DRAG ANALYSIS

(U) Where possible, drag coefficients were obtained to determine whether the turbulent drag rise location agreed with the schlieren observations as to when transition moved off the body. The data were all reduced to zero angle-of-attack values by using the usual equation:

$$C_{D_o} = C_D + C_{D_\delta}\,\overline{\delta^2}$$

(3)

The value of C_{D_δ} was established from tests in which more than one data point was obtained at a constant Reynolds number. A slope, C_{D_δ}, of $2.5/\text{radian}^2$ was used for the laminar body conditions and a slope of $3.82/\text{radian}^2$ for the turbulent body conditions. Since the average value of $\overline{\delta^2}$ was about $4.7\ \text{deg}^2$, this change amounted to about one-half-percent average correction to the data. The plot of C_{D_o} as a function of free-stream length Reynolds number is shown in Fig. 20. The Reynolds number where transition leaves the body as observed from schlieren photographs is marked in Fig. 20 and agrees very well with the drag data indication.

SECTION V
CONCLUSIONS

(∅) For the conditions of this investigation ($M_\infty = 5.2$, $T_W/T_{aw} = 0.18$, and $R_n/R_b = 0$), the following statements may be made:

1. Transition does not jump from the body to the wake downstream of the neck as the Reynolds number is decreased, but will jump into the region upstream of the neck and remain there for a wide range of Reynolds number.

2. Under the conditions investigated, the neck geometry is a strong function of Reynolds number. The neck moves downstream and increases in diameter with decreasing Reynolds number. There is a possibility that the neck does not exist for $Re_{\infty, D} < 8 \times 10^5$ under the condition of this test.

3. The neck shock, or recompression shock, weakens with decreasing Reynolds number. The initial lip shock shape does not appear to be a function of Reynolds number for the range of body Reynolds number investigated, provided it is correctly identified in the present case where only photographic observations were made.

4. The Reynolds number of the turbulent drag rise agreed very well with schlieren observations of the location of transition.

(U) These Reynolds number effects on the base flow field will have to be taken into account when designing mathematical models to describe this region. Efforts will have to be made to determine the effects of Mach number and body shape on these variables.

REFERENCES

1. Cheng, H. K. "Recent Advances in Hypersonic Flow Research." American Institute of Aeronautics and Astronautics, Vol. 1, February 1963, pp. 295-310.

2. Lykoudis, P. S. "A Review of Hypersonic Wake Studies." The Rand Corporation RM-4493-ARPA, Santa Monica, California, May 1965.

3. Wilson, L. N. "Body Shape Effects on Axisymmetric Wakes." General Motors Defence Research Laboratories GM-DRL-TR-64-02k, Santa Barbara, California, October 1964.

4. Bailey, A. B. ARO, Inc., AEDC, Private Communication.

5. Slattery, R. E. and Clay, W. G. "The Turbulent Wake of Hypersonic Bodies." American Rocket Society 17th Annual Meeting and Space Flight Exposition Preprint Number 2673-62, Los Angeles, California, November 1962.

6. Browand, F. K., Finston, M., and McLaughlin, D. K. "Wake Measurements behind a Cone Suspended Magnetically in a Mach Number 4.3 Stream." AGARD Conference Proceedings Number 19 (Preprint), Fluid Physics of Hypersonic Wakes, 64 Rue de Varenne, Paris 7e, France, May 1967.

7. Chapman, D. K., Kuehn, D. M., and Larson, H. K. "Investigation of Separated Flows in Supersonic and Subsonic Streams with Emphasis on the Effect of Transition." National Advisory Committee for Aeronautics Report 1356, Washington, D. C., 1958.

8. Lees, L. "Hypersonic Wakes and Trails." American Institute of Aeronautics and Astronautics, Vol. 2, March 1964, pp. 417-428.

9. Au, R. H. C. "An Investigation of the Compressible Laminar Wake behind a Long Slender Cylinder." University of California, College of Engineering Report AS-66-14, Berkeley, California, September 1966.

10. Murman, E. M., Peterson, C. W., and Bogdonoff, S. M. "Diagnostic Studies of Laminar Hypersonic Cone Wakes." AGARD Conference Proceedings Number 19 (Preprint), Fluid Physics of Hypersonic Wakes, 64 Rue de Varenne, Paris 7e, France.

11. Gold, H. "Stability of Laminar Wakes." Doctoral Dissertation, California Institute of Technology, Pasadena, California, 1963.

12. Waldbusser, E. "Geometry of the Near Wake of Pointed and Blunt Hypersonic Cones." American Institute of Aeronautics and Astronautics, Vol. 4, October 1966, pp. 1874-1875.

13. Waldbusser, E. "Geometry of the Near Wake of Pointed and Blunt Hypersonic Cones." General Electric Fluid Mechanics Component Data Memo 1:19, General Electric Company, Valley Forge, Pennsylvania, September 1964.

14. Ragsdale, W. C. and Darling, J. A. "An Experimental Study of the Turbulent Wake behind a Cone at Mach 5." U. S. Naval Ordnance Laboratory NOLTR 66-95, White Oak, Maryland, September 1966.

15. Hama, F. R. "Experimental Investigations of Wedge Base Pressure and Lip Shock." National Aeronautics and Space Administration TR 32-1033, Washington, D. C., December 1966.

16. Bauer, A. B. "Some Experiments in the Near Wake of Cones." American Institute of Aeronautics and Astronautics, Vol. 5, July 1967, pp. 1356-1357.
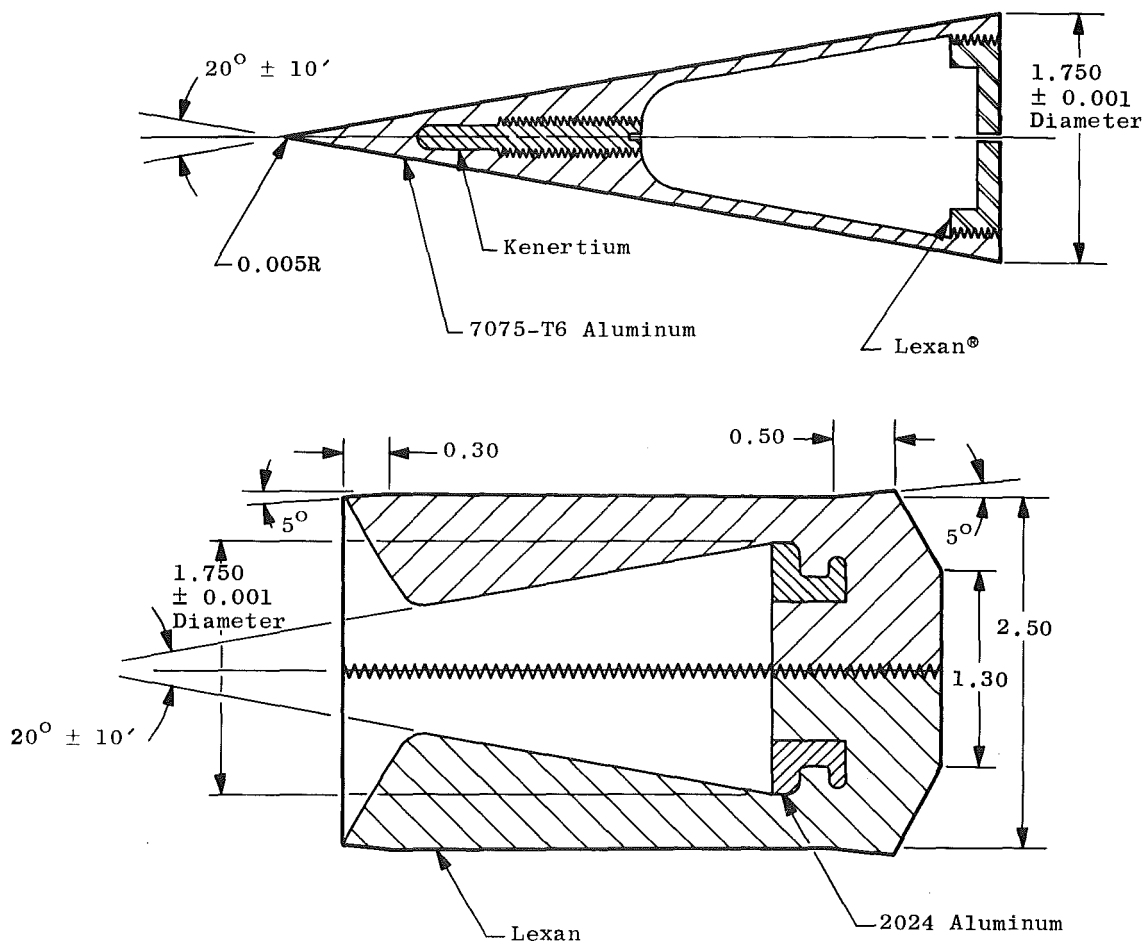
APPENDIXES
I. ILLUSTRATIONS
II. TABLES
III. DESCRIPTION OF RANGES

Fig. 1 Model A and Sabot

Dimensions are in inches.
UNCLASSIFIED

20° ± 10′

Sealed Base,
Model B₁ Only

B_1 - 1.750 ± 0.001
B_2 - 0.300 ± 0.001

7075-T6 Aluminum
4340 Steel, Rc ≥ 34
Fansteel 60 Alloy
0.005R

a. Model B₁ and B₂

20° ± 10′

0.300 ± 0.001
Diameter

0.005R
7075-T6 Aluminum

b. Model C

20° ± 10′

2024 Aluminum

Lexan

0.299
± 0.001
Diameter

0.625
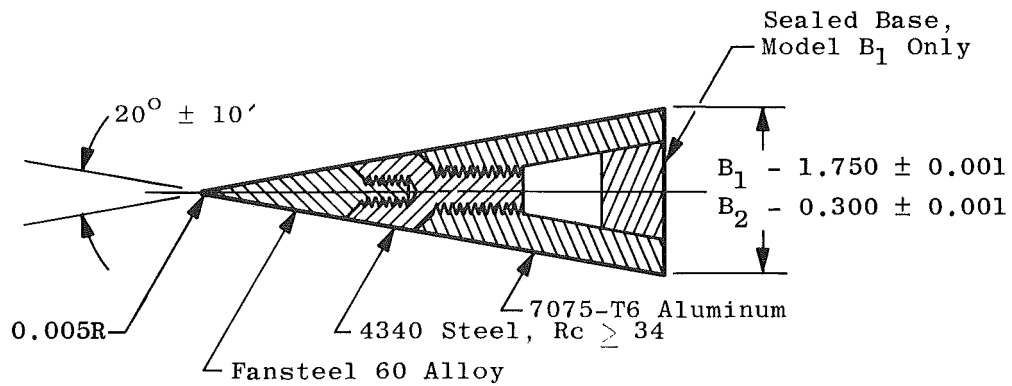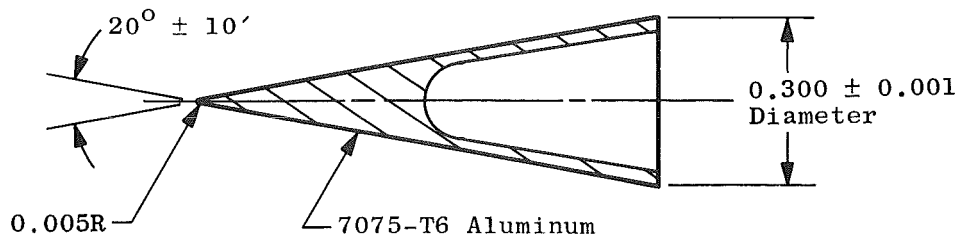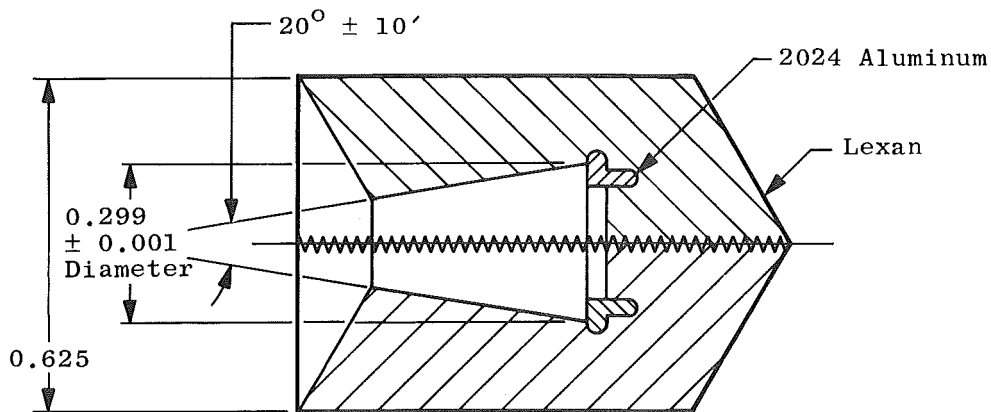
c. Sabot for Models B and C

Dimensions are in inches.

Fig. 2 Models B and C with Sabot

Turbulent Wake

Wake Shock

Leading Expansion Wave

Bow Shock

Boundary Layer

Shear Layer

w

Φ

X_{TR}

X_n
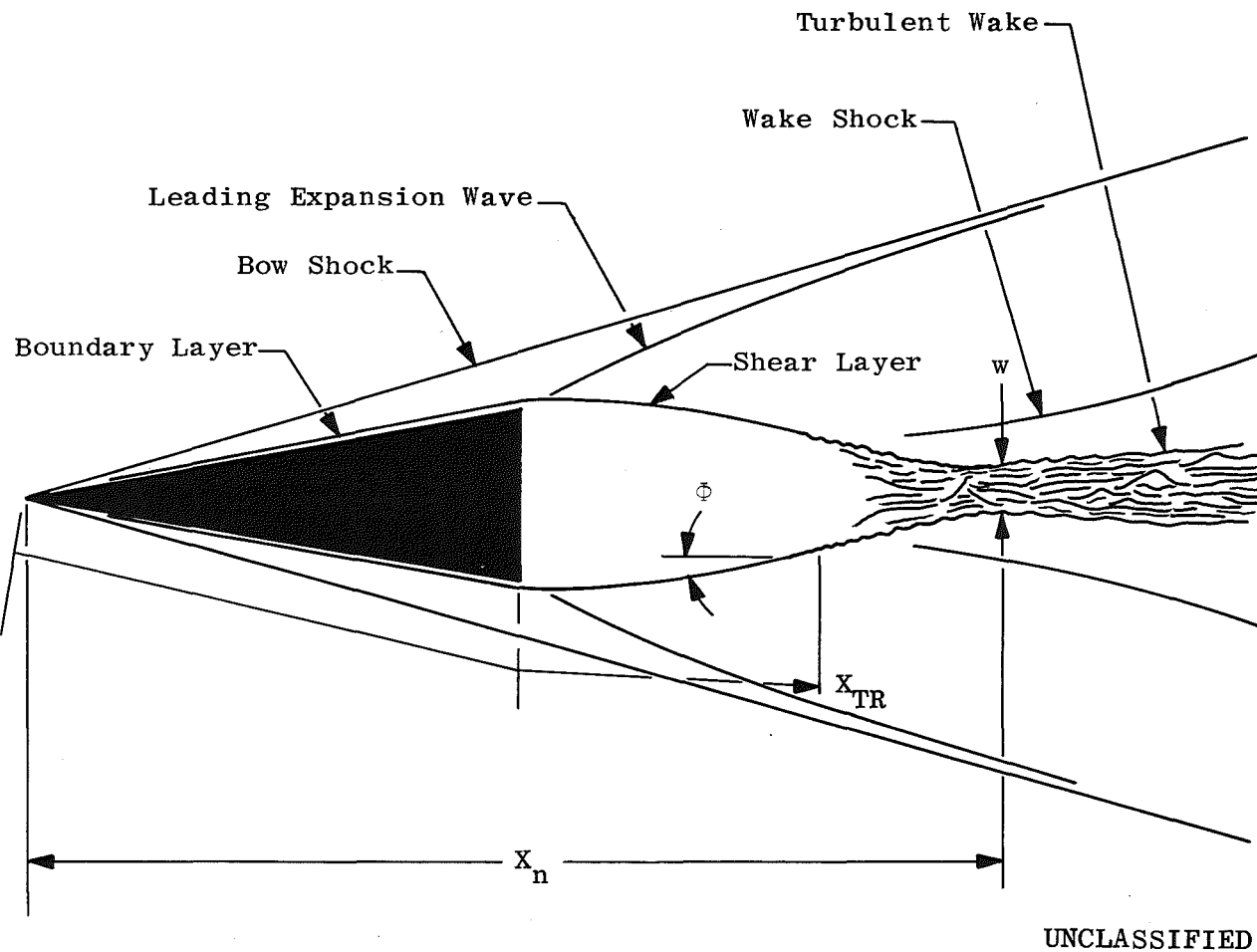
UNCLASSIFIED

Fig. 3 Sketch of the Flow Field Showing Some of the Tabulated Parameters
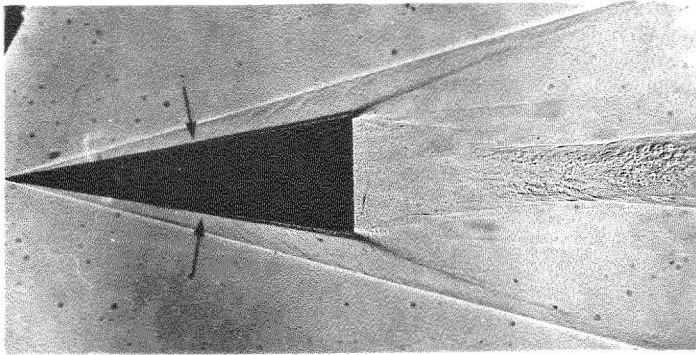
AEDC-TR-67-257

Fig. 4 Parellel-Light Shadowgram of Model A, $Re_{\infty,D}$ = 3.7 x 10^6, M_∞ = 5.1
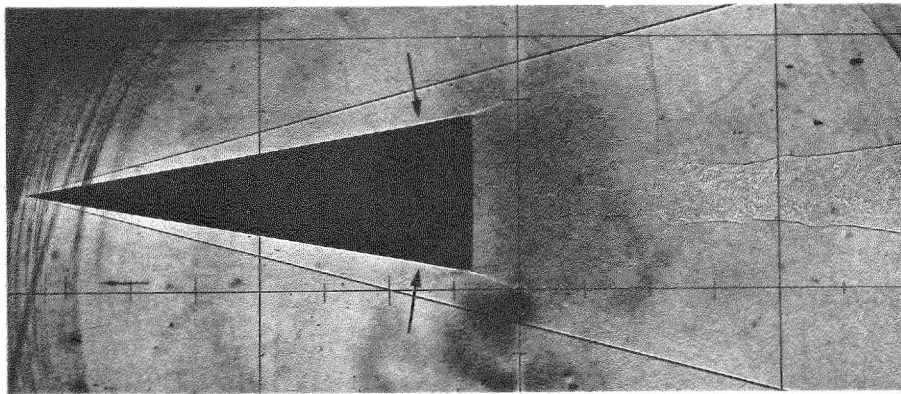
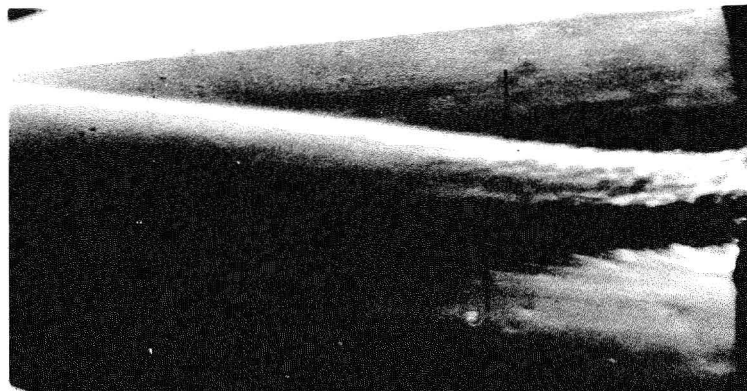Fig. 5 Point-Light-Source Shadowgram of Model A, $Re_{\infty,D}$ = 1.41 x 10^6, M_∞ = 5.3
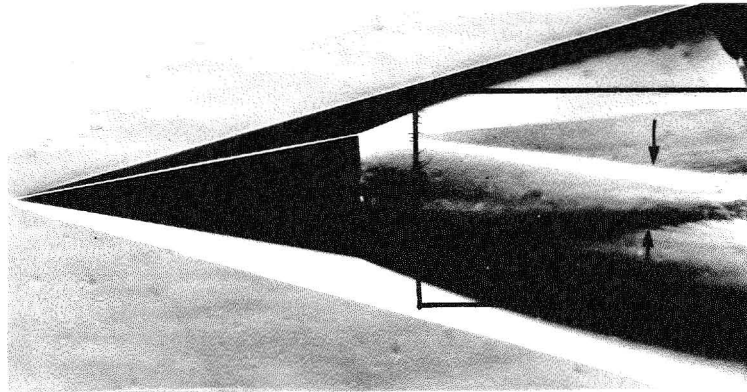
a. Photograph of Flow Field

b. Enlargement of Free Shear Layer

Fig. 6 Horizontal Knife-Edge Black-and-White Schlieren Photograph of Model A,
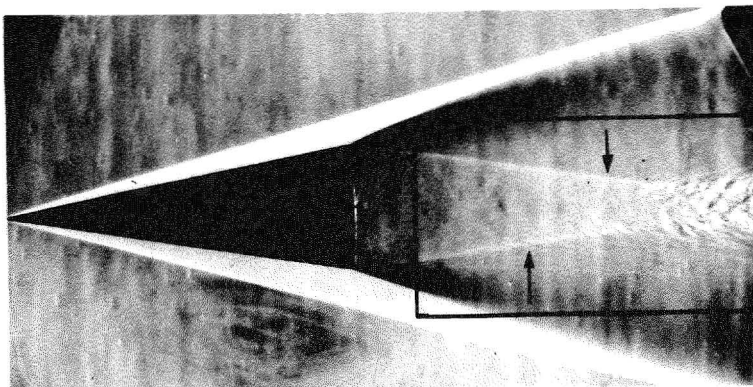$Re_{\infty, D} = 6.59 \times 10^5, M_\infty = 5.02$

a. Photograph of Flow Field
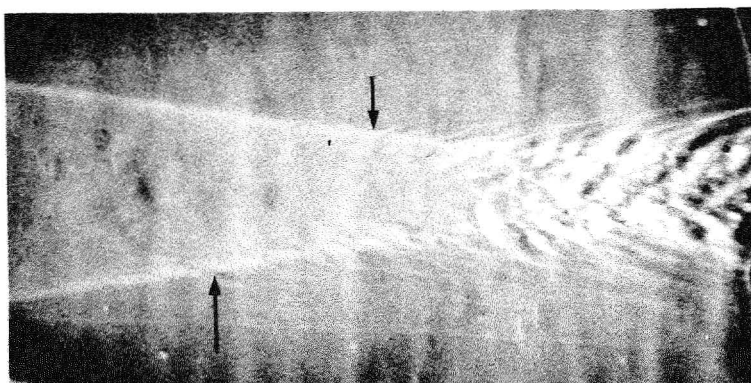
b. Enlargement of Free Shear Layer

Fig. 7 Vertical Knife-Edge Black-and-White Schlieren Photograph of Model A,
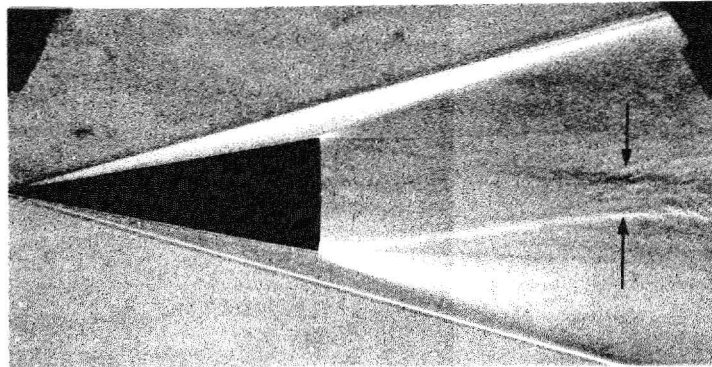$Re_{\infty,D} = 7.05 \times 10^5$, $M_\infty = 5.28$

Fig. 8 Color Schlieren Photograph of Model A,
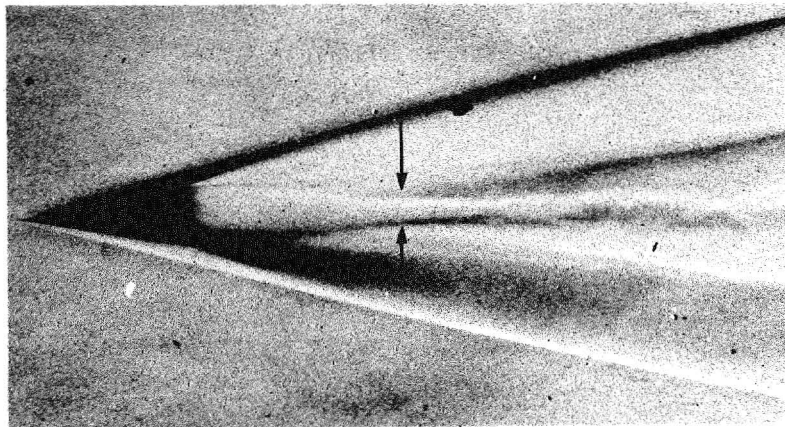$Re_{\infty,D} = 3.64 \times 10^5$, $M_\infty = 5.3$

Fig. 9 Black-and-White Schlieren Photograph of Model A,
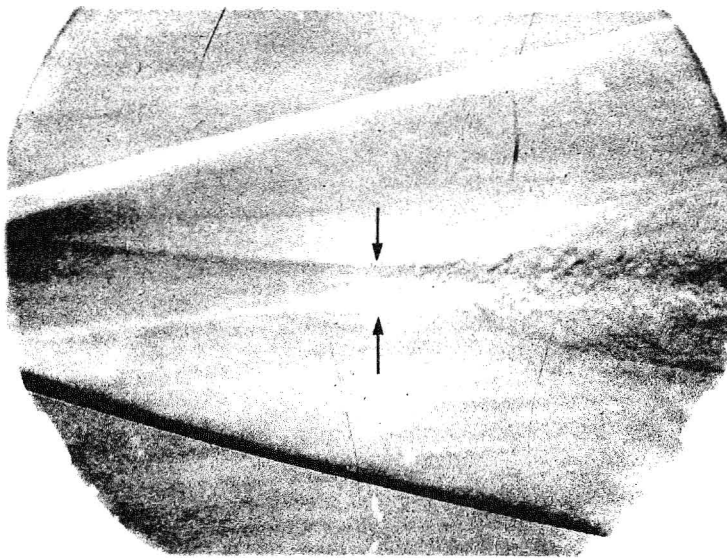$Re_{\infty,D} = 1.7 \times 10^5$, $M_\infty = 5.6$

AEDC-TR-67-257

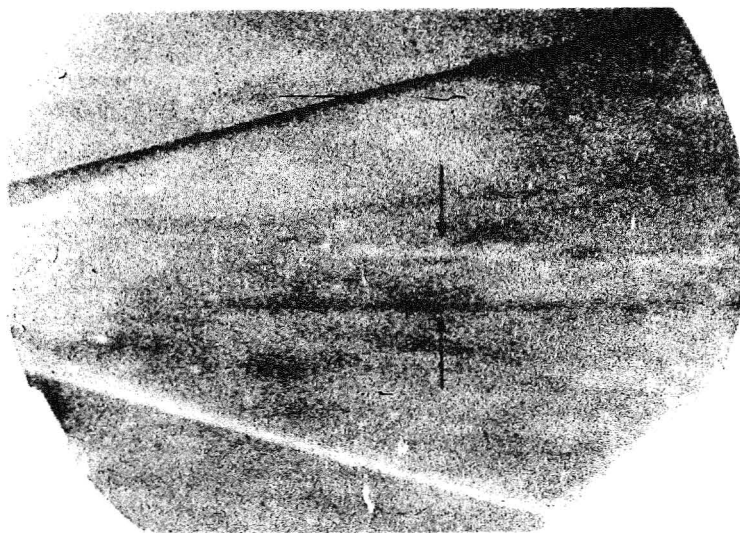Fig. 10 Color Schlieren Photograph of Model A, $Re_{\infty,D} = 1.81 \times 10^5$, $M_\infty = 5.4$

Fig. 11 Color Schlieren Photograph of Model A, $Re_{\infty,D} = 7.4 \times 10^4$, $M_\infty = 5.4$

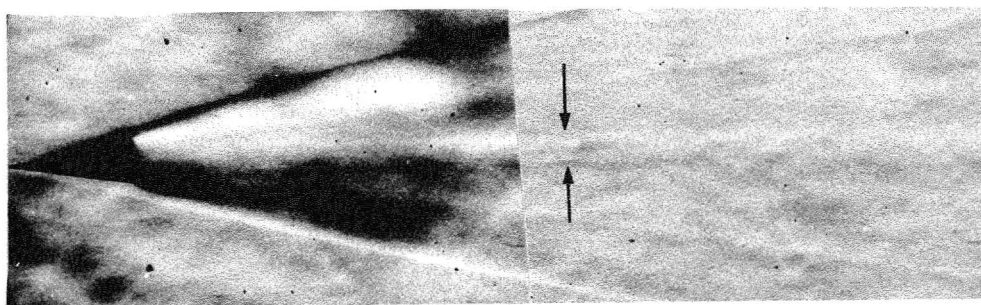DECLASSIFIED - UNCLASSIFIED

UNCLASSIFIED

Fig. 12 Two Frames of Black-and-White Drum Camera Schlieren Photograph
of Model A, $Re_{\infty,D} = 3.71 \times 10^4$, $M_\infty = 5.7$

DECLASSIFIED - UNCLASSIFIED
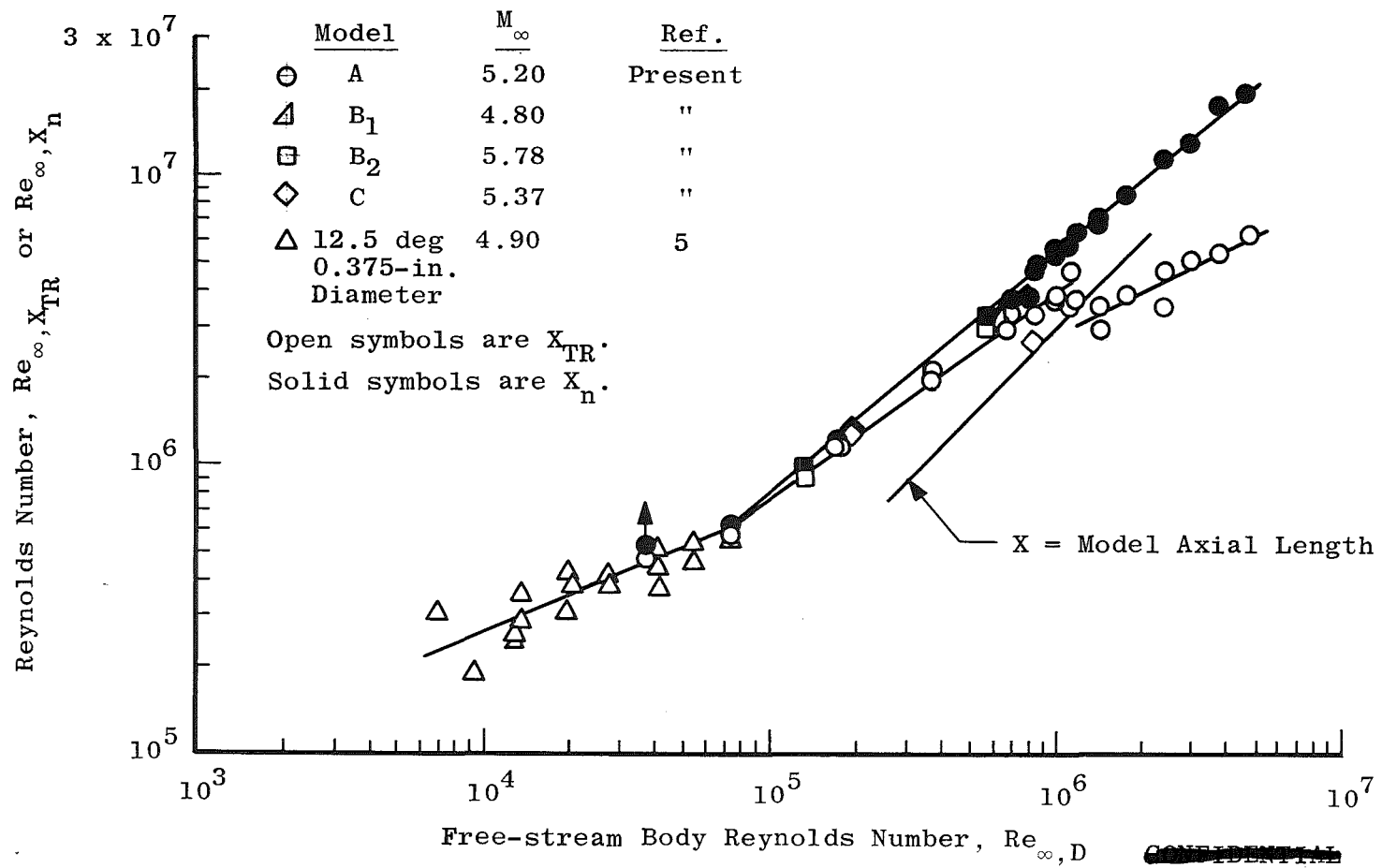
UNCLASSIFIED

Fig. 13 Variation of Transition and Neck Reynolds Numbers with Free-Stream Body Reynolds Number

UNCLASSIFIED

DECLASSIFIED / UNCLASSIFIED

UNCLASSIFIED

DECLASSIFIED / UNCLASSIFIED

a. $Re_{\infty,D} = 1.13 \times 10^6$, $M_\infty = 4.97$

b. $Re_{\infty,D} = 1.18 \times 10^6$, $M_\infty = 5.26$

c. $Re_{\infty,D} = 1.12 \times 10^6$, $M_\infty = 5.00$
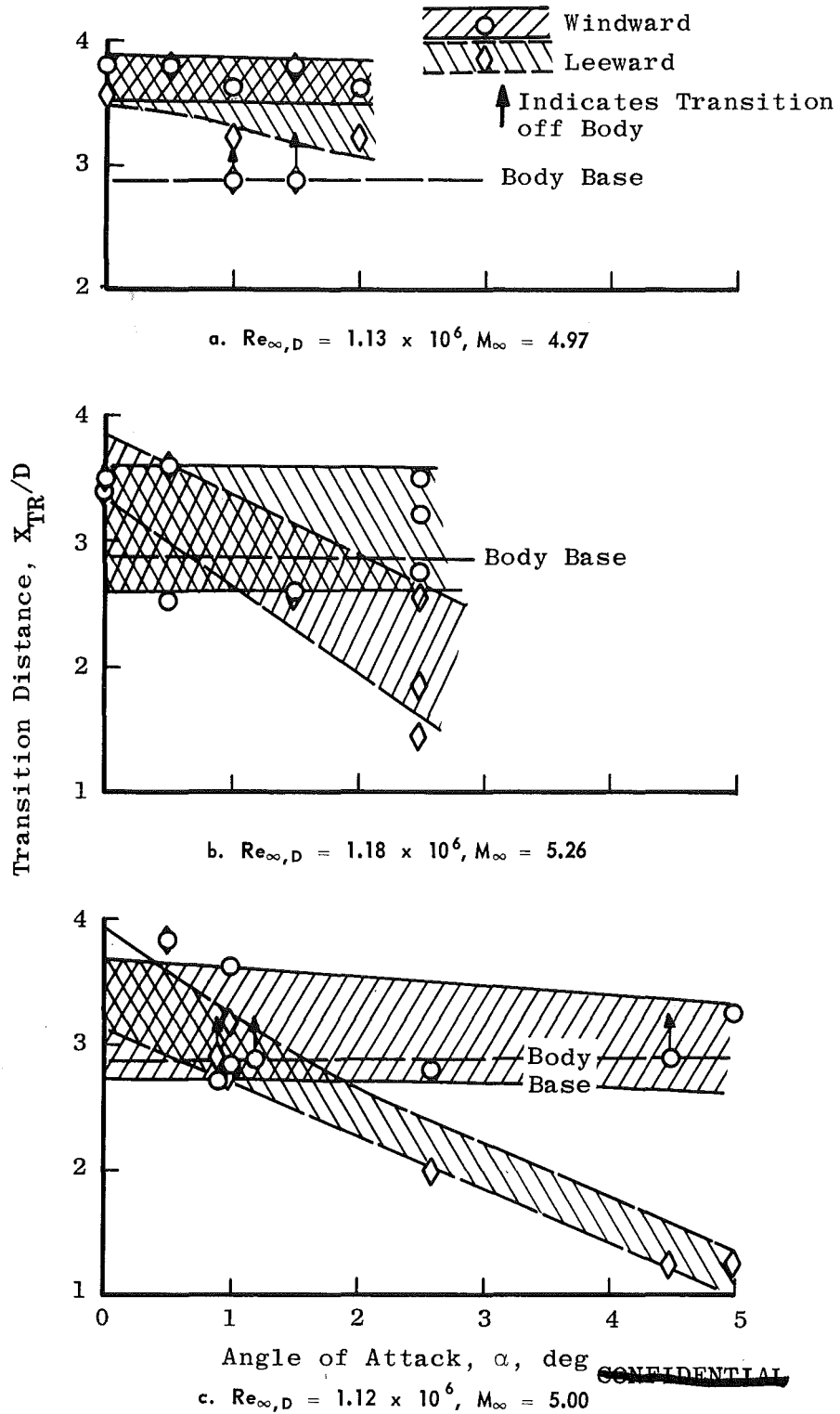
Fig. 14 Effect of Angle of Attack on Transition Distance when Transition Occurs Near to the Base for Model A
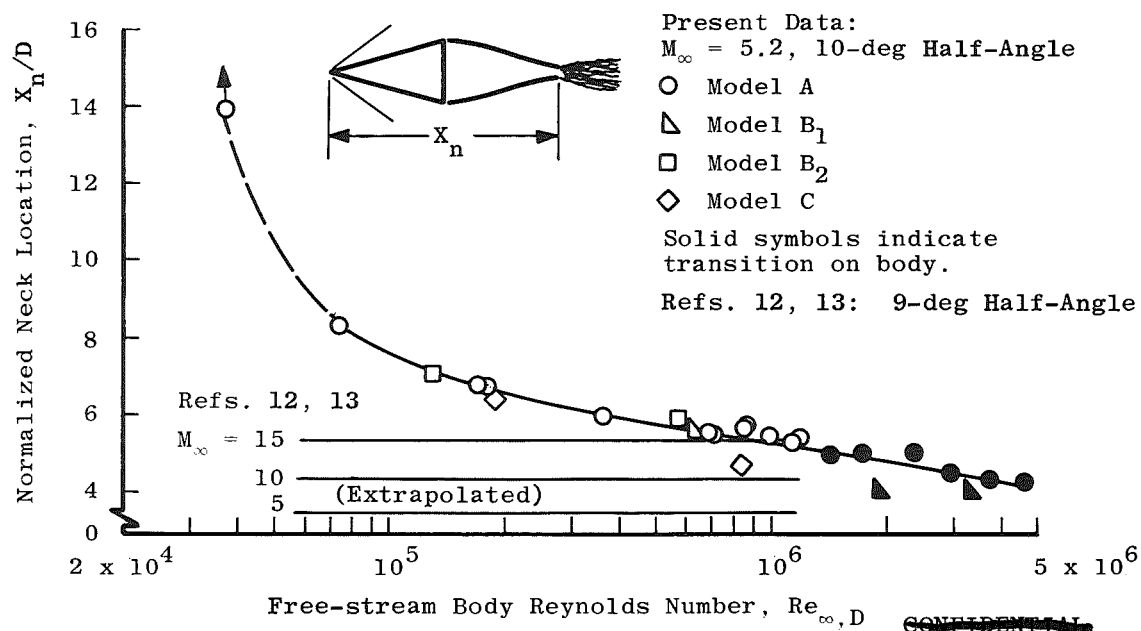
Fig. 15 Variation of Neck Location as a Function of Free-Stream Body Reynolds Number
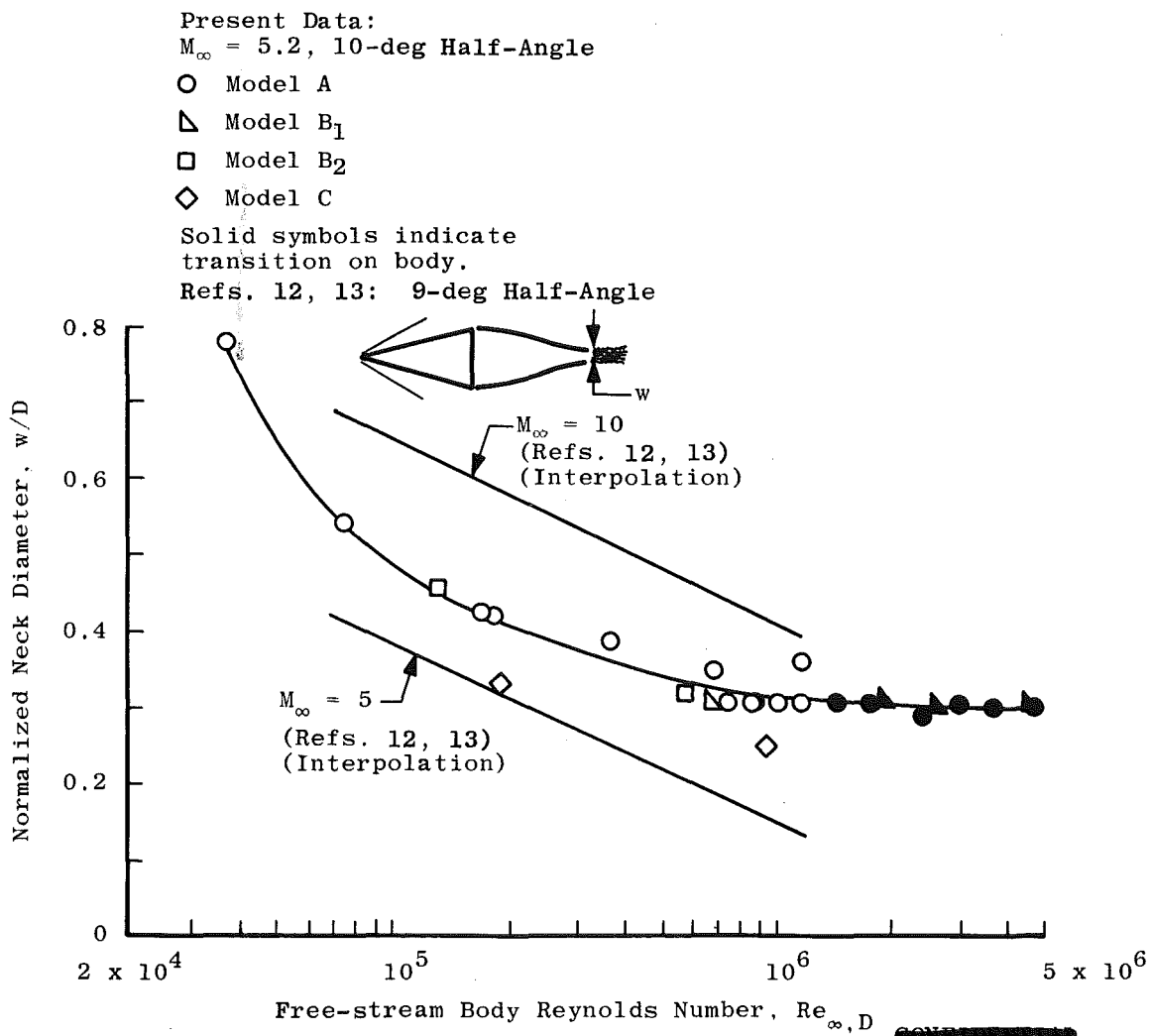
Fig. 16 Variation of Neck Diameter as a Function of Free-Stream Body Reynolds Number
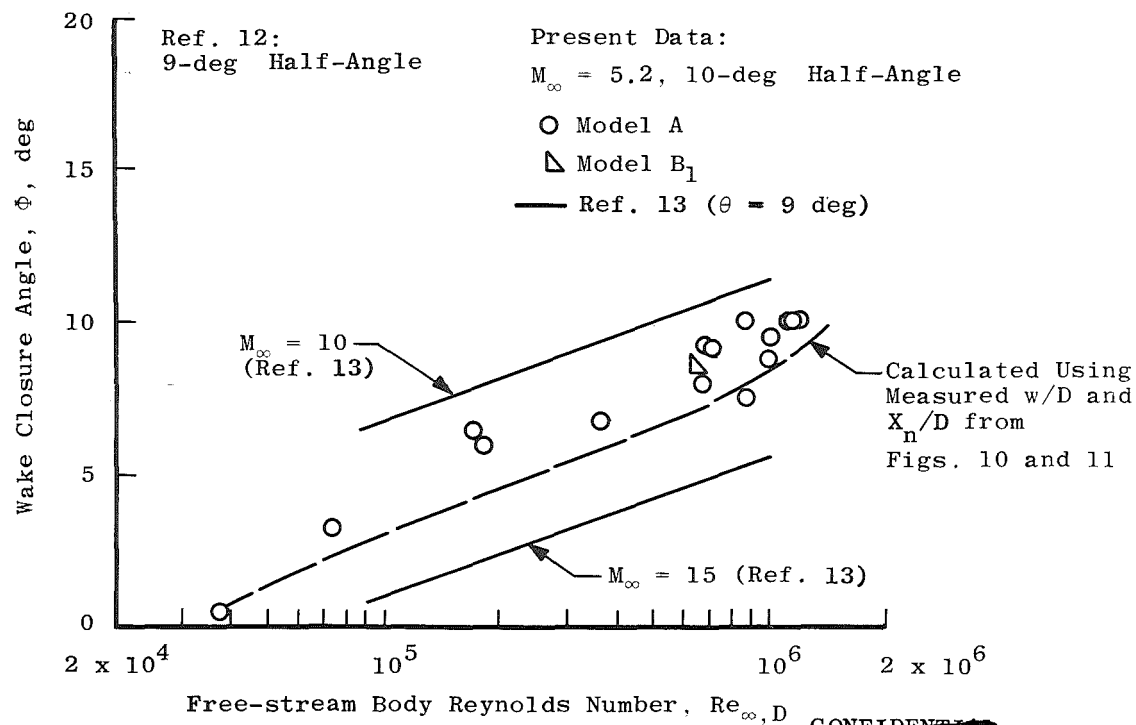
Fig. 17 Variation of Wake Closure Angle as a Function of Free-Stream Body Reynolds Number

Fig. 18 Map of the Base Flow Region

Fig. 19 Sketch of the Flow Field Showing the Base Flow Pattern for High Reynolds Number

UNCLASSIFIED

Fig. 20 Variation of Drag Coefficient with Free-Stream Length Reynolds Number

TABLE I
TEST CONDITIONS AND MEASUREMENTS

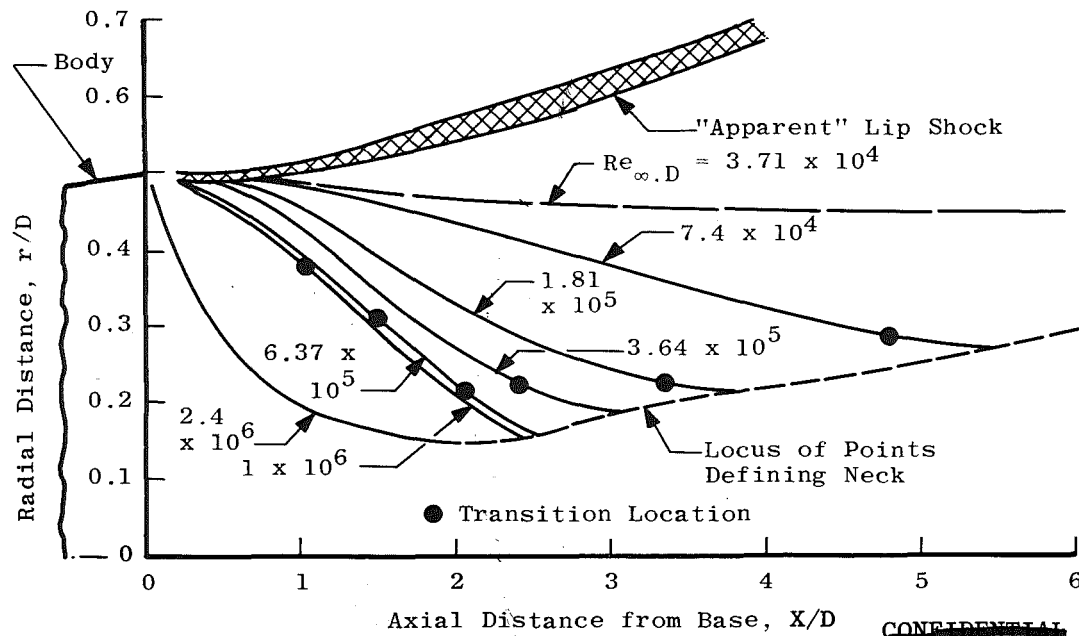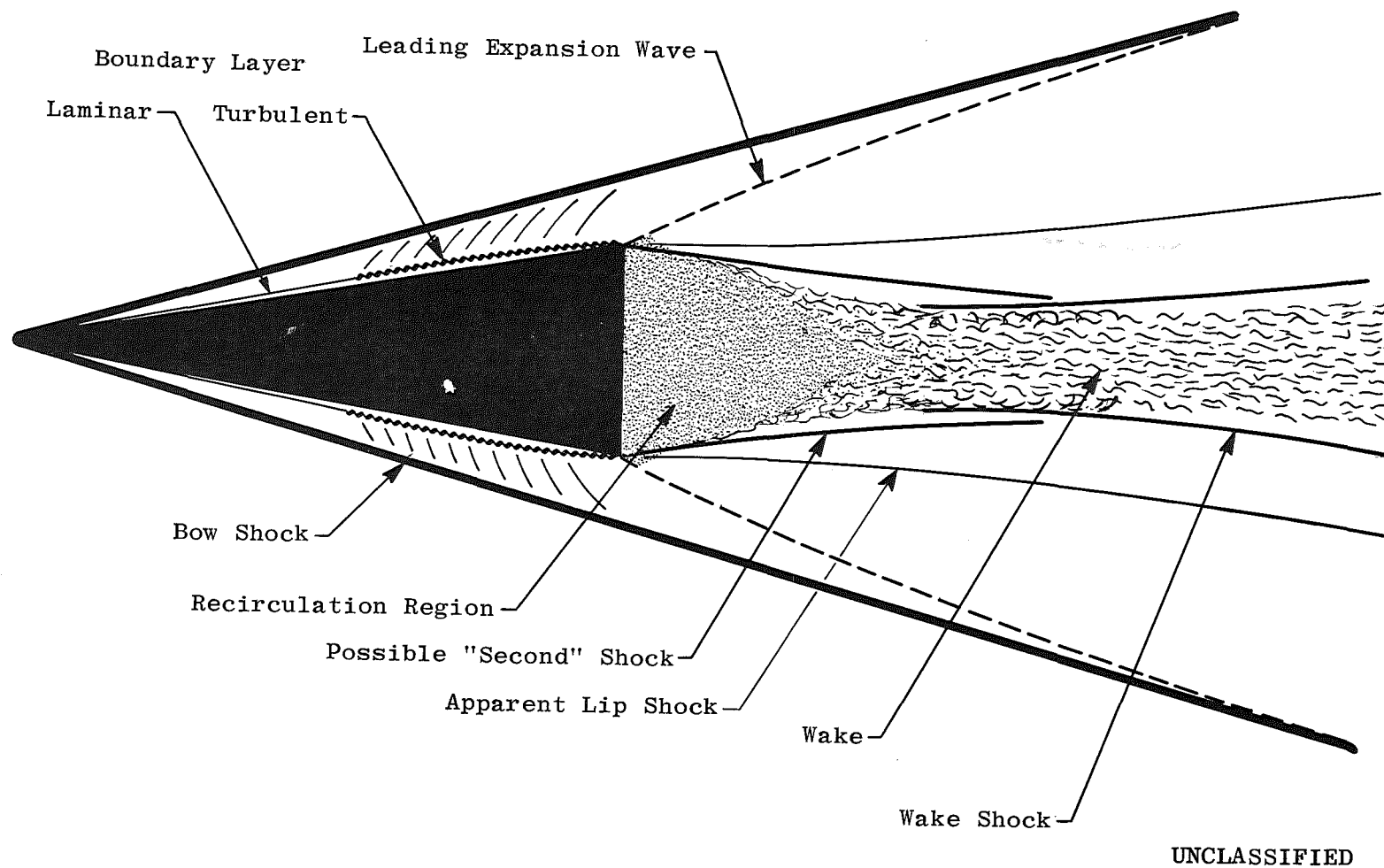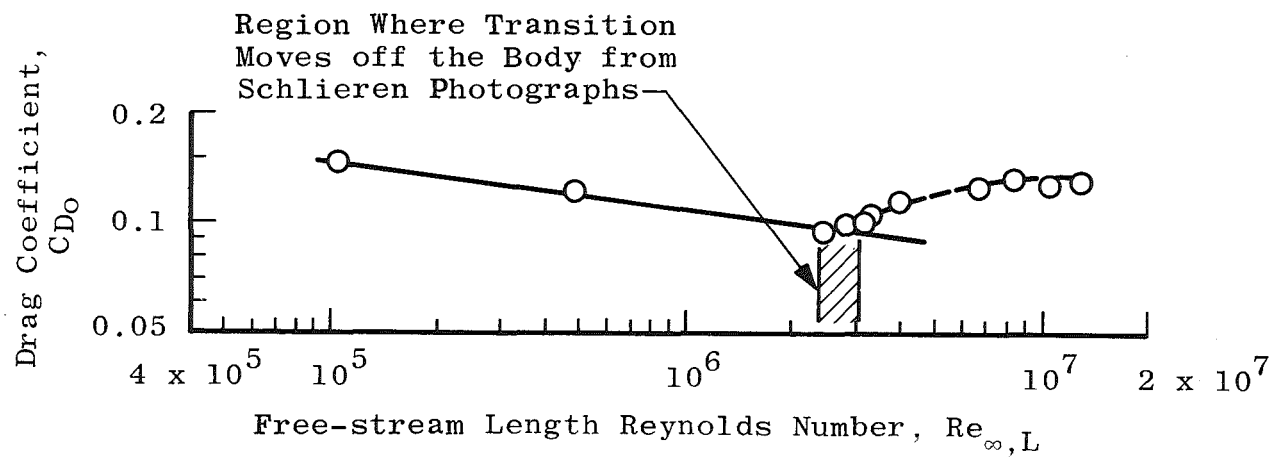| Model	M_∞	$Re_{\infty,D}$ x 10^{-5}	$\overline{\delta_2}^2$, deg	X_{TR}/D	X_n/ν	w/D	Φ, deg	C_{D_O}
A	4.78	46.4	9.83	1.37	4.30	0.30	---	0.1300
A	5.06	37.0	1.93	1.45	4.80	0.30	---	0.1296
A	4.93	29.6	3.26	1.71	4.37	0.31	---	0.1363
A	5.11	24.0	8.07	1.94	4.84	0.29	---	---
A	5.20	17.5	0.30*	2.14	4.91	0.30	---	---
A	5.32	14.1	1.46	2.48	5.03	0.30	---	0.1145
A	5.33	14.2	11.71	2.04	4.83	0.31	---	0.1145
A	5.11	8.66	0.64	3.89	5.68	0.31	7.5	0.0950
A	5.30	3.64	6.20	5.23	5.91	0.39	6.75	---
A	5.43	1.81	3.89	6.15	6.68	0.42	6.0	---
A	4.96	10.0	3.81	3.86	5.29	0.31	8.75	---
A	4.97	11.3	4.13	3.74	5.13	0.31	10.0	0.0998
A	5.06	8.45	5.23	3.86	5.53	0.31	10.0	0.1060
A	5.39	0.74	3.41	7.65	8.23	0.54	3.25	---
A	5.26	11.8	5.45	2.87	5.33	0.36	10.0	0.1065
A	5.15	6.85	6.44	4.33	5.43	0.36	8.0	---
A	5.00	10.0	3.07	3.73	5.59	0.28	9.5	0.0980
A	5.11	23.6	0.59	1.49	4.88	0.29	---	0.1276
A	5.00	11.2	6.50*	2.66	5.30	0.32	10.0	---
A	5.70	0.371	3.20	12.60	>13.83	0.78	0.5	0.1477
A	5.83	0.380	30.40	---	---	---	---	0.1477
A	5.63	1.70	11.70	6.69	6.73	0.43	6.5	0.1231
A	5.02	6.59	1.0 *	5.08	5.43	0.31	9.0	---
A	5.28	7.05	4.70	4.85	5.40	0.31	9.0	---
B_1	4.75	6.37	5.44	4.88	5.41	0.31	8.5	---
B_1	4.62	18.3	6.25*	---	4.12	0.31	---	---
B_1	5.02	33.2	6.25*	---	4.10	0.31	---	---
B_1	4.80	46.1	4.00*	---	4.22	0.31	---	---
B_2	5.76	5.71	2.75	5.23	5.74	0.32	---	---
B_2	5.80	1.31	26.99	6.80	7.18	0.46	---	---
C	5.05	8.31	5.0 *	3.17	4.58	0.25	---	---
C	5.68	1.94	10.0 *	6.43	6.50	0.33	---	---

*(angle-of-attack)^2 where read for transition location. Not enough data to establish $\overline{\delta^2}$.

APPENDIX III
DESCRIPTION OF RANGES

(U) VKF 100-ft Hypervelocity Range K. The range consists of a 100-ft-long, 6-ft-diam steel tank. A 14-ft-long, 6-ft-diam blast tank is connected to the range by a short spool piece. The sabot is stripped in this tank. For the single-stage gun launches of this experiment, the blast tank was extended 20 ft by the addition of a 14-in.-diam pipe to allow a greater sabot separation time.

(U) Range pressure was monitored with two Hass® mercury manometers and one MKS® Baratron unit. Measurement errors using this system, over the range of pressures for this test, was less than 0.062 percent of reading.

(U) Range temperature was monitored at six stations with copper-constantan thermocouples. System error was ±1.0°F.

(U) Six dual-axis spark shadowgraphs are situated at nominal 15-ft intervals along the range. Optical axes at each station are mutually orthogonal with the range centerline. The centerline field of view of these systems is 12 in. The spark light sources have an exposure duration of 0.1 μsec. Time durations which separated the shadowgraph exposures were measured by 10-mc chronographs. Timing resolution was ±0.1 μsec. Flow field information was obtained from this system for free-stream body Reynolds numbers greater than 7.0 x 10^5.

(U) A high-sensitivity, single-pass schlieren system is positioned 15 ft from the range entrance. The schlieren has a 12-in.-diam field of view. It was used as either a parallel-light shadowgraph, black-and-white schlieren, or a color schlieren system, depending on the sensitivity desired. The color system uses a light source with a duration of 0.2 μsec. The light source for the black-and-white systems has a duration of 0.1 μsec.

(U) VKF 1000-ft Hypervelocity Range G. The range consists of a 1000-ft-long, 10-ft-diam steel tank. A blast chamber, which absorbs the muzzle gases and provides a sabot trap, makes up the initial 85 ft of the range.

(U) Pressures were monitored at three stations along the range using MKS Baratron units. Measurement errors using this system did not exceed 1 percent of reading.

AEDC-TR-67-257

(U) Range temperatures were monitored at three stations using copper-constantan thermocouples. System error was ±1.0°F.

(U) Forty-three dual-axis, spark shadowgraphs are located at nominal 20-ft intervals along the range. Optical axes at each station are mutually orthogonal with the range centerline. The centerline field of view of these systems is 30 in. The spark light sources have an exposure duration of 0.12 μsec. Timing resolution between the stations is ±0.1 μsec.

(U) A high-sensitivity, single-pass schlieren system is positioned 156 ft from the range entrance. The schlieren has a 30-in.-diam field of view and is operable in either single-frame or multiframe modes. In the latter, as many as 20 frames are obtained. Exposure duration is 0.1 μsec.

DOCUMENT CONTROL DATA - R & D

(Security classification of title, body of abstract and indexing annotation must be entered when the overall report is classified)

1. ORIGINATING ACTIVITY *(Corporate author)*	2a. REPORT SECURITY CLASSIFICATION
Arnold Engineering Development Center ARO, Inc., Operating Contractor Arnold Air Force Station, Tennessee	▬▬▬▬▬▬▬
	2b. GROUP ▬▬▬▬▬

3. REPORT TITLE

EXPERIMENTAL STUDY OF FLOW GEOMETRY AND TRANSITION IN THE NEAR WAKE OF A SHARP SLENDER CONE (U)

4. DESCRIPTIVE NOTES *(Type of report and inclusive dates)*

September 1, 1966 to February 1, 1967 - Final Report

5. AUTHOR(S) *(First name, middle initial, last name)*

K. E. Koch, ARO, Inc.

6. REPORT DATE	7a. TOTAL NO. OF PAGES	7b. NO. OF REFS
April 1968	39	16

8a. CONTRACT OR GRANT NO.	9a. ORIGINATOR'S REPORT NUMBER(S)
AF 40(600)-1200 b. PROJECT NO. 8953	AEDC-TR-67-257
c. Program Element 6240533F	9b. OTHER REPORT NO(S) *(Any other numbers that may be assigned this report)*
d. Task 895309	N/A

10. DISTRIBUTION STATEMENT In addition to security requirements which must be met, this document is subject to special export controls and each transmittal to foreign governments or foreign nationals may be made only with prior approval of AEDC (AETS), Arnold Air Force Station, Tennessee.

11. SUPPLEMENTARY NOTES	12. SPONSORING MILITARY ACTIVITY
Available in DDC	Arnold Engineering Development Center (AETS), Air Force Systems Command, Arnold Air Force Sta., Tenn

13. ABSTRACT

This is a report of an investigation of the near wake of a supersonic sharp cone in free flight in an aeroballistics range. Data concerning transition location and near wake geometry have been obtained.

(U)

This document is subject to special export controls and each transmittal to foreign governments or foreign nationals may be made only with prior approval of Arnold Engineering Development Center (AETS), Arnold Air Force Station, Tennessee.

DD FORM 1473
1 NOV 65

14. KEY WORDS	LINK A		LINK B		LINK C	
	ROLE	WT	ROLE	WT	ROLE	WT
wake studies						
cones						
supersonic flow						
flow geometry						
transition						